博士論文

Ultrastrong and Superelastic Nanolaminate Aerogels

（ナノ層状構造に基づく超剛性かつ超弾性のエアロゲル）

孫 志方

Introduction

Aerogels are lightweight, 3D nanoporous materials composed mostly of air.[1] Since the first report of aerogel in 1931, the unique structures and properties of aerogels have attracted many attention from material fields. Furthermore, from more practical viewpoints, the extremely low thermal conductivity of aerogels promises their application as ecofriendly alternatives of fossil fuel-based polymer foams, which are widely used as heat-insulation materials for construction. However, conventional aerogels are generally very weak and brittle. The networks of aerogels are usually composed of interconnected hard nanoparticles including silica nanoparticles, and upon compression of aerogels, cracks can be generated and quickly propagate in the networks, leading to the collapse of aerogels. As the most easy approach for strengthening such aerogels, hybridization of the interconnected hard particles with organic polymers have been attempted several times so far, but all the resultant materials undergo plastic deformation upon compression.[2] Alternatively, thin and flexible nano-filaments, such as carbon nanotubes, have been employed as the components in place of hard nanoparticles, where the entanglement of the nano-filaments often afford elastic networks. However, the compressive strength of such aerogels is extremely low.[3] Recently, a particular class of silica aerogels, which were prepared from alkyl-substituted trifunctional silanes in place of tetrafunctional silanes, partially realized strength and elasticity, although they were still too brittle and plastic under repeated or large compressive strain.[4] Thus, none of the aerogels reported so far can simultaneously fulfill high mechanical strength and high elasticity, which are essential for the science and technology of aerogels to phase. Indeed, simultaneous pursuit of strength and elasticity remains a ground challenge in the field of structural materials, particularly for lightweight porous materials such as aerogels.[5]

As represented by nacres and bones, some biological materials in nature exhibit exceptional toughness, even though they are composed solely of individually brittle components. The key design principle of such biomaterials is hierarchical nanolaminated structure, which efficiently suppresses the propagation of cracks and also enhances the interfacial interactions between building blocks, leading to the toughening of materials. Inspired by such biological materials, the author hypothesized that aerogel networks can be likewise strengthened by fabricating into nanolaminated structures. Recently, Aida *et al.* found that an aqueous dispersion of atomically thin 2D crystals, titanate nanosheets (TiNSs, Scheme 1a),[6] can be cofacially aligned in a magnetic field to form a huge monodomain structure, in which TiNSs are arranged into a layered structure with a uniform and large plane-to-plane separation of several hundred nanometers.[7] Consequently, a numerous number of nanolaminated spaces are created by the confinement with TiNSs. We testify our hypothesis by in-situ hydrogelation of a methylated silane source (MS; Scheme 1b) within a pre-formed TiNS nanolaminated matrix to form a nanolaminated composite hydrogel (MS/TiNS^{lam} hydrogel; Scheme 1c). Solvent exchange and subsequent supercritical CO_2 drying afforded a nanolaminated aerogel (MS/TiNS^{lam} aerogel; Scheme 1c, i). Thus obtained MS/TiNS^{lam} aerogel exhibited unprecedentedly excellent mechanical properties, with

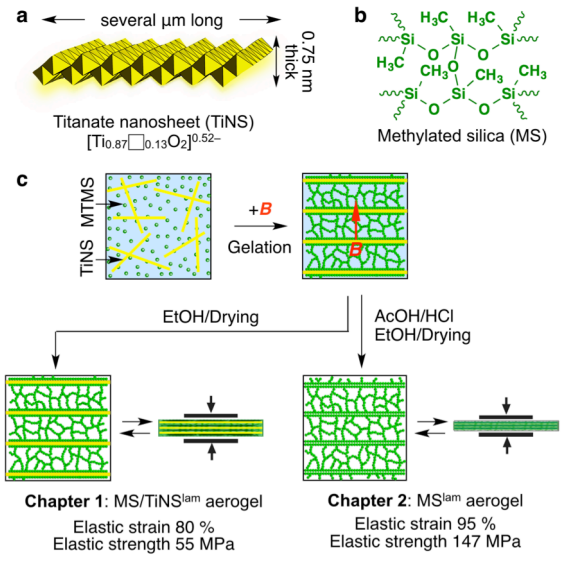

Scheme 1. Schematic representation for the preparation of the ultrastrong and superelastic nanolaminate aerogels: (1) MS/TiNS^{lam} aerogel and (2) MS^{lam} aerogel.

simultaneously realizing strength and elasticity; upon compression, perfectly elastic deformation was possible up to high compression stress (>55 MPa) and strain (>80%) with excellent fatigue resistance (>100 cycles of 80% strain), as described in detail in Chapter 1. For further improvement of the mechanical properties and pursuit of the toughening mechanism, the author developed another type of nanolaminated aerogel (MS^{lam} aerogel; Scheme 1c, ii) by etching TiNS in $MS/TiNS^{lam}$ hydrogel followed by solvent exchange and supercritical drying. Surprisingly, MS^{lam} aerogel exhibited even remarkable mechanical properties; MS^{lam} could be compressed up to 95% strain without losing its elasticity, where the stress reached to no less than 147 MPa. Even though the maximally compressed state was comparable to bulk nonporous silica, MS^{lam} aerogel could fully spring back to its original shape when the compression force was released. The details are described in Chapter 2. Contrary to other reinforced aerogels, the nanolaminated aerogels $MS/TiNS^{lam}$ aerogel and MS^{lam} aerogel retained all the excellent intrinsic properties of silica aerogels, such as low density, high porosity, high surface area, and low thermal conductivity. The discoveries in this dissertation illustrate how the nanolamination can change the properties of aerogel networks composed of interconnected hard nanoparticles, leading to aerogels with exceptionally high strength and elasticity. The author also emphasizes that the striking mechanical properties of the present aerogels would bring a paradigm shift in the field of low-density materials, where it has long been believed that high strength and high elasticity are trade-off and there is no feasible way to simultaneously achieve them.

Chapter 1. Development of Nanolaminate Aerogels Containing Titanate Nanosheets

Nanolaminate structures are ubiquitous in nature, such as nacres, bones and plants, which can effectively toughen the materials and make them crack-resistant. The author obtained inspiration from these biological materials to use the nanolaminate structure for toughening aerogels. As described in the introduction part, TiNSs dispersed in water can be cofacially aligned in a magnetic field to form nanolaminated confined spaces with a regular thickness of ~100 nm.[6] On the other hand, it was recently reported that methylated silica aerogels (MS) made from a trifunctional silica source (methyltrimethoxysilane; MTMS) show much higher flexibility compared with the conventional silica aerogels made from tetrafunctional silica sources (*e.g.* TEOS). In the present study, the author attempted to form the nanolaminated MS network by the polycondensation of MTMS within the confined spaces between magnetically oriented TiNSs in water (Scheme 1c, i). Typically, the MTMS was first hydrolyzed in aqueous diluted acid solution to form reactivated methylated silane ($CH_3Si(OH)_3$). After mixing with a surfactant (pluronic F-127) and TiNS, the mixture was subject to a 10-T magnetic field at 20 °C so that TiNSs were unidirectionally oriented. Over a period of 3 days, in-situ polycondensation of the reactive methylated silane proceeded within the nanolaminated spaces confined between TiNSs to afford $MS/TiNS^{lam}$ hydrogel. Through solvent exchange with ethanol and supercritical CO_2 drying, $MS/TiNS^{lam}$ hydrogel was converted into $MS/TiSN^{lam}$ aerogel. As references, the corresponding aerogels without TiNS (MS aerogel) and with randomly oriented TiNSs ($MS/TiNS^{ran}$ aerogel) were likewise prepared, by omitting the addition of TiNSs and the

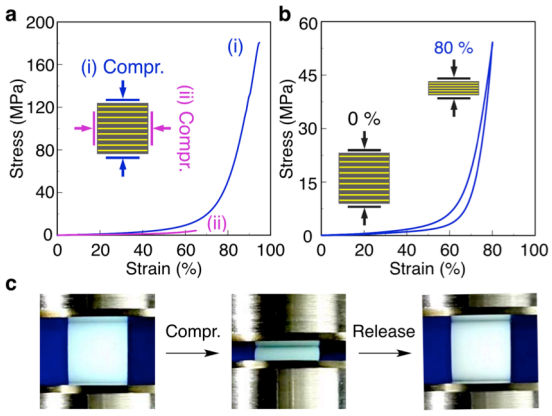

Figure 1. (a) Anisotropic mechanical property of $MS/TiNS^{lam}$ aerogel. (b) Elastic property of $MS/TiNS^{lam}$ aerogel when compressed to 80% strain. (c) Sequential photos showing the spring-back behavior of the $MS/TiNS^{lam}$ aerogel after compression to 80%.

application of the magnetic field, respectively. All the aerogels show characteristic properties of usual aerogels, such as low density (0.18 g cm^{-3}), high porosity (>90%), and high surface area (~430 m^2 g^{-1}).

Anisotropic structure of MS/TiNS^{lam} aerogel was confirmed by various analytical methods. When observed along the applied magnetic field, MS/TiNS^{lam} aerogel appeared shiny white due to light reflected by TiNSs, while in the orthogonal direction, it showed translucent blue color due to the Mie scattering from the silica network. In the Scanning electron microscopy (SEM) images of the cross section orthogonal to the applied magnetic field, several flat, in-plane oriented nanosheets peeped through the nanofibrillar network of silica particles with a diameter of ~15 nm. Contrary to this, in the cross section parallel to the magnetic flux direction, only the silica network was observed, in consistent with the thickness of TiNSs (0.75 nm) that is under the resolution of SEM. 2D small angle X-ray scattering (2D SAXS) on the precursor hydrogel, MS/TiNS^{lam} hydrogel, with beams orthogonal to the TiNS plane generated only a single diffuse spot, whereas parallel to the TiNS plane produced a linear array of multiple diffuse spots up to the (11 0 0) face, indicating that TiNS aligns with a uniform plane-to-plane separation of 89.7 nm. All the above measurements confirm the periodic nanolaminate structure in MS/TiNS^{lam} aerogel.

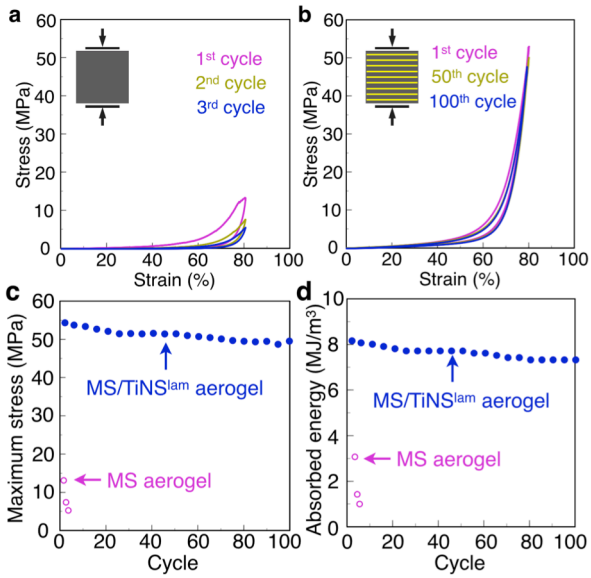

Figure 2. (a), (b) Stress-strain curves of selected cycles during repeated compression to 80% of (a) MS aerogel, (b) MS/TiNS^{lam} aerogel. (c) Maximum stress and (d) absorbed energy of MS and MS/TiNS^{lam} aerogel with respect to number of cycles.

The compression tests revealed that MS/TiNS^{lam} aerogel show excellent mechanical properties toward compression. When a mechanical force was applied in the direction orthogonal to the TiNS plane, MS/TiNS^{lam} could be compressed up to 95% without fracture (Figure 1a, i), although partial plastic deformation was inevitably accompanied at 90–95% strain. At the strain of 95%, the stress reached to 180 MPa, which was one of the highest values among aerogels ever reported so far. For realizing such excellent mechanical properties, TiNSs should play a crucial role, because the reference aerogel free from TiNS (MS aerogel) underwent larger plastic deformation at relatively low strain and stress, indicating poor strength and elasticity (data not shown). In addition, the relative angle between the applied mechanical force and the TiNS plane is crucial. When compressed in the direction parallel to the TiNS plane, MS/TiNS^{lam} aerogel fractured at 59% strain with a compressive strength of 4.5 MPa (Figure 1a, ii). In relation to this, MS/TiNS^{ran} aerogel also underwent larger plastic deformation or even break at relatively low strain and stress (data not shown).

Although MS/TiNS^{lam} aerogel underwent partial plastic deformation at 90–95% strain, the resultant aerogel remained partially elastic and sprang back to ~50% of its original length when released from the compression. This observation motivated the author to estimate the strain region for MS/TiNS^{lam} aerogel to undergo perfectly elastic deformation. As shown in Figure 2b, MS/TiNS^{lam} aerogel was perfectly elastic up to 80% strain. Worth noting is that the stress at 80% strain reached to no less than 55 MPa, which is two orders of magnitude higher than the state-of-the-art elastic aerogels based on carbon materials, and *ca.* 4 times larger than MS aerogel (Figure 2a). Furthermore, upon repeated compression, MS/TiNS^{lam} aerogel

showed excellent fatigue-resistance. Even after 100 cycles of compression up to 80% strain, the maximum stress decreased only by 9% from the original value, and only 1.9% of plastic deformation occurred (Figure 2c, blue). Furthermore, the deterioration occurred mainly at the initial 3 cycles, and the following 97 cycles hardly changed the mechanical properties of MS/TiNS^{lam} aerogel. It should also be noted that MS/TiNS^{lam} aerogel absorbed huge energy (8.1 MJ m^{-3}) during one cycle of compression at 0–80% strain, which is the highest among all elastic aerogels ever reported so far and indicates a wide range of application as energy dissipation, cushioning and packaging materials *etc.* In sharp contrast, MS aerogel could retain its elasticity only at the first cycle and then rapidly degraded at the second and third cycles (Figure 2c and 2d, purple).

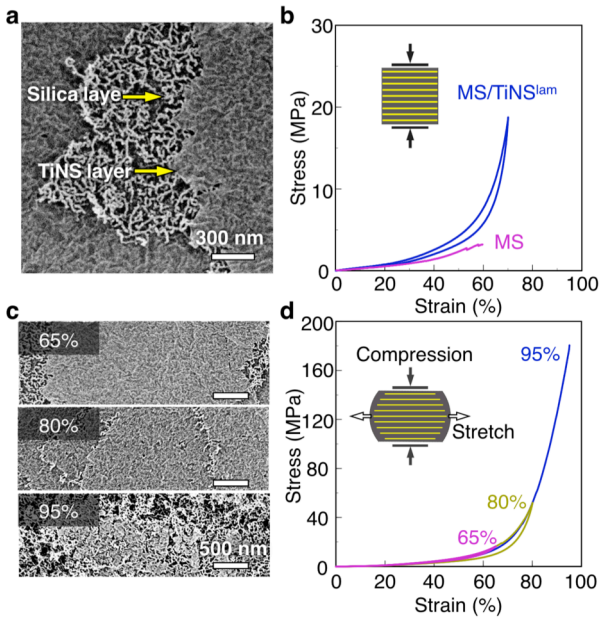

Figure 3. (a) SEM image of MS/TiNS^{lam} aerogel. (b) Stress-strain curves of notched aerogels. (c) SEM images and (d) stress-strain curves of MS/TiNS^{lam} aerogel after compressed to 65%, 80% and 95%.

The excellent fatigue resistance of MS/TiNS^{lam} aerogel might be attributed to the nanolaminated structure (Figure 3a), which is generally known to efficiently dissipate energy and suppress crack propagation. To clarify this point, the author investigated the notch tolerance of MS/TiNS^{lam} aerogel. Thus, by using a sharp needle, a hole with a diameter of 0.6 mm and a length of 8.0 mm was perforated at the center of a cube-shaped MS/TiNS^{lam} aerogel with dimensions of 10 × 10 × 10 mm. The notched sample was then compressed in the direction parallel to the hole. As shown in Figure 3b, MS/TiNS^{lam} aerogel could be compressed to 70% and fully sprang back, showing the maximum stress of 18.7 MPa. Collapse of the sample started to occur only when the applied strain was increased to 80%. In sharp contrast, notched MS aerogel fractured when compressed to 60% strain, with a low stress of 3.2 MPa.

For further clarifying the mechanism of how the nanolaminated structure toughens MS/TiNS^{lam} aerogel, the morphology of MS/TiNS^{lam} aerogel after compression was investigated by SEM with systematically varying the strain. Within the strain region of 0–80%, where MS/TiNS^{lam} aerogel undergoes perfectly elastic deformation, 2D shape of TiNSs in the aerogel hardly damaged (Figure 3c and 3d). However, when compressed up to 95%, where significant plastic deformation of MS/TiNS^{lam} aerogel occurs, TiNSs were broken into small pieces. We attribute the breakage of TiNS to the expansion of nanosheets in the direction of its plane upon compression (poison's ratio 0.1), which can greatly enhance the stress. Once the strain reaches to the limitation, TiNS breaks. Therefore, the key to these outstanding mechanical performances is the alternate nanolaminates of silica network and TiNSs, which synergistically strengthen the network and sufficiently suppresses the crack propagation once generated inside.

Chapter 2. Development of Nanolaminate Aerogels Free of Titanate Nanosheets

In Chapter 1, the author demonstrated that the alternate nanolaminates of silica network and TiNSs can synergistically strengthen the composites aerogel, making it ultrastrong and superelastic. However, several points are still elusive, such as the role of silica nanolaminate and the structural differences between the silica networks of MS and MS/TiNS^{lam} aerogels. The author envisioned that, if the TiNS in the MS/TiNS^{lam} aerogel can be selectively etched, the resultant material would be helpful to understand the mechanism on how the silica nanolaminates affect the mechanical properties in the MS/TiNS^{lam} aerogels. Bearing this in mind, the author discovered a method, using corrosive acid (CH_3CO_2H:HCl = 9:1, v/v), to selectively dissolve TiNSs in MS/TiNS^{lam} hydrogel. After repeated washing with ethanol and supercritical drying, a nanolaminate aerogel composed of only MS, named as MS^{lam} aerogel, can be prepared (Scheme 2).

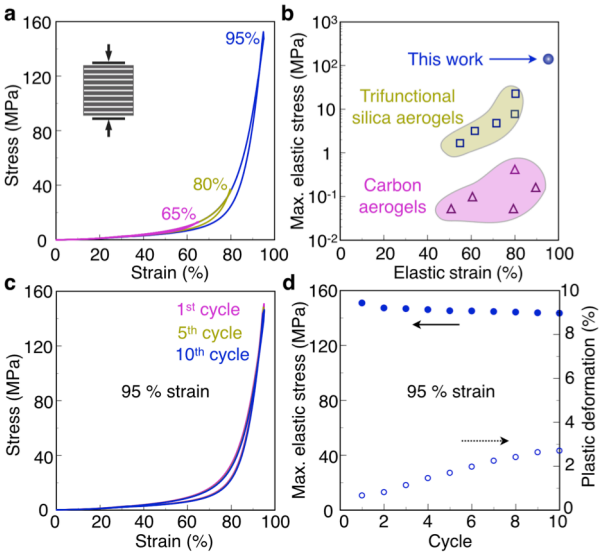

Figure 4. (a) Stress-strain curves of MS^{lam} aerogel at various strains. (b) Ashby chart plotting maximum elastic stress versus maximum elastic strain for the MS^{lam} and other previously reported aerogels. (c) Stress-strain curves of the selected cycles during repeated compression to 95% of the MS^{lam} aerogel. (d) History of maximum elastic stress and plastic deformation for the MS^{lam} aerogel during repeated compression at 80% strain.

Cyclic compression tests of MS^{lam} aerogel were conducted at varying strain ranges from 0–65%, 0–80% and 0–95%. To our surprise, the MS^{lam} aerogel underwent perfectly elastic deformation up to 95% strain and fully sprang back to its original shape when released from the compressive force (Figure 4a). Such a large elastic strain region has never been observed before for nanoporous materials (Figure 4b). Furthermore, the maximum stress applicable to MS^{lam} aerogel (at 95% strain) reaches to 147 MPa, which is one order higher than MS aerogels (at 80% strain) and around 3 times larger than the MS/TiNS^{lam} aerogel (at 80% strain). Repeated cyclic compression tests suggested that MS^{lam} aerogel is highly durable to this ultralarge strain, and retain 95% of its maximum stress after 10 cycles (Figure 4c and 4d). The absorbed energy per cycle of MS^{lam} aerogel was 8 times larger than MS aeroegel and 3 times larger than MS/TiNS^{lam} aerogel. Thus, by using nanolaminated structure, the author developed an unprecedented aerogel composed solely of silica, which exhibit both ultrahigh strength and superelasticity never achieved before. Considering the porosity and density of the aerogel, the compressive strain of 95% is close to the theoretical limit. Thus, upon compression to 95% strain, the aerogel becomes like monolithic solids, in terms of porosity and density. The perfect spring back from such a condensed state is quite surprising.

Why the nanolaminate aerogel has simultaneously high compressive strength and high elastic strain? To address this issue, the author systematically investigated the structural characteristics of the MSlam aerogels. During the sol-gel process of the MS/TiNS^{lam} gel, polycondensation takes place within the confined spaces of the TiNS nanolaminates, in which the distance is 90 nm. Because the tetramethylammonium counterions on the TiNS can catalyze the polycondensation of silica, a MS layer first grows onto the TiNS, and further polycondensation proceeds to fill the remaining confinements of 60 nm, which can only accept 4 MS particles. Thus, numerous struts formed, which can be regarded as the pillars (Figure 5a). Upon compression of MS^{lam} aerogel, the nano-pillars can enhance the modulus, and longer silica nanofibers has less structural defects to initiate the cracks. Even some cracks generated inside the MS^{lam}

network, the nanolaminate structure can efficiently suppress their propagation, making the MS^{lam} aerogel superelastic (Figure 5b). To further prove the role of silica nanolaminates, morphology of the MS^{lam} aerogel was investigated by the SEM before and after compression to 95% strain. Before compression, MS^{lam} aerogel had a well-connected, continuous long nanofibrillar network (Figure 5c). After compression by 95% strain, the network remained intact and showed no notable difference (Figure 5d). The excellent mechanical properties of MS^{lam} aerogel is attributable to such continuous network with less structural defects, which might be originated from the template effects of the TiNSs during the *in situ* hydrogelation of silica. Therefore, the key to these outstanding mechanical performances is the nanolaminate structures of the silica network, which can sufficiently suppress the crack propagation once generated inside the aerogel networks.

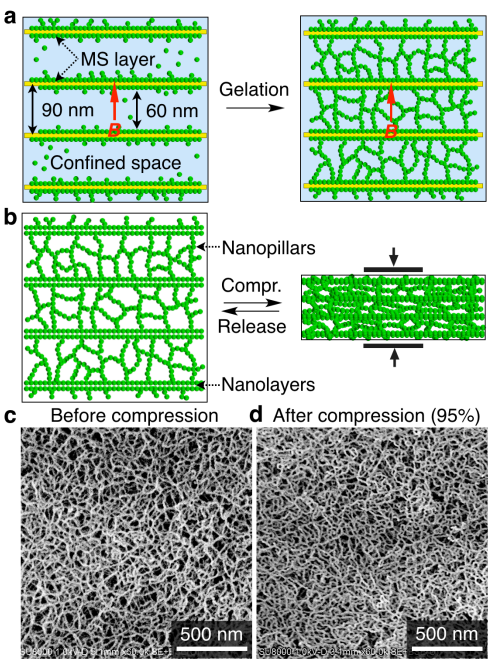

Figure 5. (a) The growth and gelation of silica network during the sol-gel process of the MS^{lam} gel. (b) Upon compression, silica struts confined in nanolaminates efficiently boost the modulus, and cracks can be suppressed by the MS nanolaminates. (c,d) SEM images of the MS^{lam} aerogel before (c) and after (d) being compressed by 95% strain.

Summary

The author succeeded in developing unprecedented nanolaminate aerogels with concurrent ultrahigh strength and ultralarge elasticity, as well as excellent fatigue resistance. Besides, in contrast to conventional silica network, the nanolaminate aerogels can retain excellent mechanical properties even when notched. Furthermore, the nanolaminated aerogels can retain all the excellent intrinsic properties characteristic of silica aerogels, such as low-density, high porosity, high surface area and low thermal conductivity. The present discoveries are significantly important in the following aspects: (i) Utility of nanolaminate structures for toughening materials is clarified. (ii) An exception is posed for the preconceived notion that high strength and high elasticity are trade-off for low-density materials. (iii) General problems of aerogels that hamper their practical use are shown to be resolved by proper material design.

References

[1] Kistler, S. S. *Nature* **1931**, *127*, 741.
[2] Meador, M. A. B. *et al. Chem. Mater.* **2005**, 17, 1085–1098.
[3] Kim, K. H. *et al. Nat. Nanotech.* **2012**, *7*, 562–566.
[4] Kanamori, K. *et al. Adv. Mater.* **2007**, 19, 1589–1593.
[5] Cao, A. *et al. Science* **2005**, 310, 1307–1310.
[6] Sasaki, T. *et al. J. Am. Chem. Soc.* **1996**, *118*, 8329–8335.
[7] Liu, M. *et al. Nature* **2015**, *517*, 68–72.